

Explicit imaging expressions for weak horizontal transverse isotropy

Vigen Ohanian PGS, Thomas M. Snyder LLCC, Jose M. Carcione OGS*

SUMMARY

Despite the recognized prevalence of vertical parallel cracks in reservoir rocks, the necessary imaging expressions for the weak HTI (horizontal transverse isotropy) system have not been studied in sufficient generality. With the exception of the P-wave phase velocity formula, the existing first-order HTI expressions are restricted to certain regimes of applicability.

The HTI and VTI (vertical TI) systems are distinguished from one another merely by the way they are configured in relation to the acquisition coordinate system. In this paper, using coordinate transformation rules connecting the two systems, we first map all the coordinate dependent physical quantities appearing in the imaging VTI expressions, to their HTI counterparts - the mapped quantities are accurate to first-order. Then, by a simple substitution into the VTI expressions, we develop a complete suite of imaging expressions for systems with weak HTI.

Our P- and S-wave phase velocity, polarization, and group velocity expressions are entirely general, in that they account for wave propagation in arbitrary directions within the HTI media. Thus, they can be readily incorporated into the multi-component production processing algorithms.

INTRODUCTION

Closed form phase velocity, polarization vector and group velocity expressions, describing the propagation of elastic waves in isotropic and anisotropic media, are the basic ingredients of elastic imaging algorithms used in seismic exploration. Group velocity formulas allow the computations of converted wave travel-time tables used in the Kirchhoff migration algorithms. For anisotropic imaging purposes, the reflected energy must be constructed by superposition of plane waves – where each plane wave is characterized by its own anisotropic phase velocity and polarization vector (Ohanian, Snyder, and Carcione, 1997). The suite of expressions representing phase velocities, polarizations and group velocities for P- and S-waves, hereafter, will be referred to as the “imaging expressions”.

The HTI system is commonly used for modeling parallel vertical cracks, which are replete in the earth’s crust. Shear-wave splitting technology is an effective tool for the determination of fracture orientations in reservoir rocks (Lynn et al 1995). Ohanian et al (1992) developed a two step shear-wave splitting algorithm, consisting of a downward continuation step and a matrix diagonalization step, which was shown to unravel depth variant fracture

orientations from vertical seismic profiling (VSP) data. This downward continuation algorithm was also shown to be formally equivalent to the layer-stripping algorithm of Winterstein et al (1991).

While solutions to the problem of vertical propagation of elastic waves in the HTI system (used in VSP) are well understood, and have been successfully integrated into reservoir characterization algorithms, existing elastic imaging expressions capable of handling wave propagation in arbitrary directions within such media are incomplete and lack generality. The only available HTI imaging expression that meets the extent of generality needed in surface seismic exploration is the first-order P-wave phase velocity formula derived by Gajewski et al (1996) – their expression indeed shows the explicit dependence on phase and polar angles. Tsvankin (1997) showed the equivalence between the VTI media and the symmetry-axis plane of the HTI media, and provided relations between the VTI and the HTI sets of Thomsen parameters.

To be able to properly process finite-offset multi-component surface-seismic data acquired over vertically fractured rocks, the basic imaging expressions must necessarily be able to account for propagation in arbitrary directions with respect to the acquisition coordinate system.

The HTI and VTI systems are members of the same crystal symmetry class known as the hexagonal symmetry. The two systems are distinguished from one another merely by the way they are configured in relation to the acquisition coordinate system. (Figure 2 illustrates each configuration). Therefore, all wave propagation expressions in HTI are related to their VTI counterparts through an appropriate coordinate transformation.

Our strategy for deriving the first-order elastic imaging expressions for the HTI system, directly from the well-known VTI expressions, is illustrated in Figure 2 where the VTI and the HTI coordinate systems are superimposed over the same medium with hexagonal symmetry. To derive the desired expressions we do three things: (a) we first establish the appropriate coordinate transformation rules between the two systems. (b) Then, we obtain first-order HTI representations for each of the coordinate-dependent physical quantities appearing in the VTI imaging expressions. (c) Finally, by substituting the HTI representations of these quantities into the VTI imaging expressions we arrive at the corresponding HTI formulas. Our P-wave phase velocity expression agrees with Gajewski et al (1996).

Explicit imaging expressions for weak horizontal transverse isotropy

The standard geophysical acquisition coordinate system has its z-axis oriented perpendicularly to the earth's surface and increases downward. For our analysis we find it convenient to choose the x-axis to be along the symmetry axis of the HTI system (Figure 2b). A simple rotation about the z-axis will take an arbitrary surface-acquisition system to our (x,y,z) system. To facilitate the representation of polarization vectors and group velocities for waves with wave-vector \vec{k} , we introduce the spherical-coordinates $(\hat{\theta}, \hat{\phi}, \hat{k})$ as shown in Figure 1. \hat{k} is a unit vector in the direction of \vec{k} .

Weak anisotropy parameters

For weak anisotropy, instead of dealing explicitly with individual elastic constants, it is convenient to work with some naturally defined "weak anisotropy parameters" (WAPs) that would apply uniformly to the VTI and HTI systems. We now review the following widely used WAPs associated with TI systems.

The VTI system:

Figure 2a illustrates the VTI system, which is fully described by C_{33}, C_{44} , and the following set of three WAPs:

$$\begin{aligned} \varepsilon = g_{11} &= \frac{C_{11} - C_{33}}{2C_{33}}, & \gamma = g_{66} &= \frac{C_{66} - C_{44}}{2C_{44}}, \\ \delta = g_{13} &= \frac{C_{13} + 2C_{44} - C_{33}}{C_{33}}. \end{aligned} \quad (1)$$

where, ε and γ are Thomsen parameters (1986). The parameter δ was discussed by Gajewski (1996) and by Ohanian (1996).

The HTI system:

Figure 2b illustrates the HTI system. The HTI system is fully described by C_{33}, C_{44} , and the following set of three WAPs:

$$\begin{aligned} \varepsilon = g_{11} &= \frac{C_{11} - C_{33}}{2C_{33}}, & \gamma = g_{66} &= \frac{C_{66} - C_{44}}{2C_{44}}, \\ \delta^* = g_{13} &= \frac{C_{12} + 2C_{66} - C_{33}}{C_{33}}. \end{aligned} \quad (2)$$

where, ε and γ are the same as their VTI counterparts. The parameter δ^* was discussed by Gajewski et al (1996).

Imaging expressions for weak VTI

For reference, in what follows, we show the well-known VTI imaging expressions. Throughout this paper, the subscripts, p , qS , and pS will correspond to quasi-P, quasi-S and pure-S modes, respectively.

First-order polarization vectors for weak VTI:

$$\begin{aligned} \hat{u}_p &= \hat{k} + \left(\frac{C_{33}(2g_{11}\sin^2\theta + g_{13}\cos 2\theta)\sin 2\theta}{2(C_{33} - C_{44})} \right) \hat{\theta} \\ \hat{u}_{qS} &= \hat{\theta} - \left(\frac{C_{33}(2g_{11}\sin^2\theta + g_{13}\cos 2\theta)\sin 2\theta}{2(C_{33} - C_{44})} \right) \hat{k} \\ \hat{u}_{pS} &= \hat{\phi} \end{aligned} \quad (3)$$

With $g_{11} = \varepsilon$, $g_{13} = \delta$, and $g_{66} = \gamma$, the above polarization vectors agree with those of Rommel (1994) and Ohanian (1996).

First-order phase velocities for weak VTI:

$$\begin{aligned} v_p &= v_p^0(1 + g_{11}\sin^4\theta + g_{13}\sin^2\theta\cos^2\theta) \\ v_{qS} &= v_s^0\left[1 + \frac{C_{33}}{C_{44}}(g_{11} - g_{13})\sin^2\theta\cos^2\theta\right] \\ v_{pS} &= v_s^0(1 + g_{66}\sin^2\theta) \end{aligned} \quad (4)$$

Here, $v_p^0 = \sqrt{C_{33}/\rho}$ and $v_s^0 = \sqrt{C_{44}/\rho}$ where ρ is the mass density of the medium. Via $g_{11} = \varepsilon$, $g_{13} = \delta$, and $g_{66} = \gamma$, the above results agree with Thomsen (1986).

First-order group velocities for weak VTI:

$$\begin{aligned} \vec{V}_p &= v_p \hat{k} + v_p^0(2g_{11}\sin^2\theta + g_{13}\cos 2\theta)\sin 2\theta \hat{\theta} \\ \vec{V}_{qS} &= v_{qS} \hat{k} + v_s^0\left(\frac{C_{33}}{2C_{44}}\right)(g_{11} - g_{13})\sin 4\theta \hat{\theta} \\ \vec{V}_{pS} &= v_{pS} \hat{k} + v_s^0 g_{66} \sin 2\theta \hat{\theta} \end{aligned} \quad (5)$$

where, v_p , v_{pS} and v_{qS} refer to the phase velocities given in (4).

Rules for transforming VTI to HTI

To derive first-order elastic imaging expressions for the HTI system, directly from the corresponding VTI expressions, we will need to transform each of the coordinate-dependent quantities appearing in equations (3) through (5) into their HTI counterparts. These quantities are the polar and azimuth angles (θ, ϕ) , the unit vectors $(\hat{\theta}, \hat{\phi})$, the stiffness coefficients C_{ij} , the weak anisotropy parameters g_{ij} , and the phase velocities (v_p^0, v_s^0) . By substituting the HTI counterparts of these quantities into the VTI imaging expressions we will thus arrive at the corresponding HTI expressions. In this section, all quantities denoted by tilde belong to the HTI system.

Explicit imaging expressions for weak horizontal transverse isotropy

Transformation of the coordinate systems:

In Figure 2c the VTI system is defined by the coordinate system $(\hat{x}, \hat{y}, \hat{z})$ while the second coordinate system $(\tilde{x}, \tilde{y}, \tilde{z})$ defines the HTI medium. (θ, ϕ) will denote the polar and azimuth angles of \hat{k} with respect to the VTI coordinate system; whereas, $(\tilde{\theta}, \tilde{\phi})$ are the polar and azimuth angles of \hat{k} with respect to the HTI coordinate system. ($\tilde{\theta}$ is the angle between \hat{k} and the \tilde{z} -axis; $\tilde{\phi}$ is the azimuth angle of \hat{k} about the \tilde{z} -axis.) Therefore, the two coordinate systems bear the following relationships:

$$\begin{aligned}\hat{x} &= \tilde{z} \\ \hat{y} &= -\tilde{y} \\ \hat{z} &= \tilde{x}\end{aligned}\quad (6)$$

Transformation rules for the polar and azimuth angles:

$$\begin{aligned}\cos \theta &= \cos \tilde{\phi} \sin \tilde{\theta}, \quad \sin \theta = \tilde{n}, \\ \cos \phi &= \frac{\cos \tilde{\theta}}{\tilde{n}}, \quad \sin \phi = -\frac{\sin \tilde{\phi} \sin \tilde{\theta}}{\tilde{n}}\end{aligned}\quad (7)$$

where, the explicit form of \tilde{n} , in terms of polar and azimuth angles $(\tilde{\theta}, \tilde{\phi})$, is defined to be

$$\tilde{n} = \sqrt{1 - \cos^2 \tilde{\phi} \sin^2 \tilde{\theta}} \quad (8)$$

Transformation rules for the unit vectors:

$$\begin{aligned}\hat{\theta} &= -\frac{\cos \tilde{\phi} \cos \tilde{\theta}}{\tilde{n}} \hat{\theta} + \frac{\sin \tilde{\phi}}{\tilde{n}} \hat{\phi} \\ \hat{\phi} &= -\frac{\sin \tilde{\phi}}{\tilde{n}} \hat{\theta} - \frac{\cos \tilde{\phi} \cos \tilde{\theta}}{\tilde{n}} \hat{\phi} \\ \hat{k} &= \hat{k}\end{aligned}\quad (9)$$

Transformation rules for elastic stiffness coefficients:

Since, in this coordinate transformation we are interchanging the x and the z axes, the following changes in the Voigt indices are in order:

$$1 \rightarrow 3 \quad 2 \rightarrow 2 \quad 3 \rightarrow 1 \quad 4 \rightarrow 6 \quad 5 \rightarrow 5 \quad 6 \rightarrow 4 \quad (10)$$

Therefore, the correspondences between the elastic moduli defined in the two systems are:

$$C_{33} = \tilde{C}_{11} \quad C_{44} = \tilde{C}_{66} \quad C_{66} = \tilde{C}_{44} \quad C_{13} = \tilde{C}_{13} \quad (11)$$

Transformation rules for WAPs

$$g_{11} = -\tilde{g}_{11}, \quad g_{66} = -\tilde{g}_{66}, \quad g_{13} = (\tilde{g}_{13} - 2\tilde{g}_{11}) \quad (12)$$

These parameter transformation rules agree, to first order, with those defined by Tsvankin (1997).

Transformation rules for "isotropic" phase velocities:

$$v_p^0 = \tilde{v}_p^0 (1 + \tilde{g}_{11}) \quad , \quad v_s^0 = \tilde{v}_s^0 (1 + \tilde{g}_{66}) \quad (13)$$

$$\text{with } \tilde{v}_p^0 = \sqrt{\tilde{C}_{33}/\rho} \quad , \quad \tilde{v}_s^0 = \sqrt{\tilde{C}_{44}/\rho}$$

Imaging expressions for weak HTI

By substituting the VTI to HTI transformation formulas (6) through (13) into the VTI imaging expressions (3), (4) and (5), we obtain the following first-order HTI imaging expressions. In these final HTI expressions we *choose to drop the tilde notation*. Thus, all expressions below refer to HTI with coordinate system as shown in Figure 2b.

First-order polarization vectors for weak HTI:

$$\begin{aligned}\hat{u}_p &= \hat{k} + \frac{C_{33}[2g_{11}(1-n^2) + g_{13}(2n^2-1)]\cos\phi\sin\theta}{C_{33}-C_{44}} \\ &\quad (\cos\phi\cos\theta\hat{\theta} - \sin\phi\hat{\phi}) \\ \hat{u}_{qS} &= -\frac{\cos\phi\cos\theta}{n}\hat{\theta} + \frac{\sin\phi}{n}\hat{\phi} + \\ &\quad \left(\frac{C_{33}[2g_{11}(1-n^2) + g_{13}(2n^2-1)]n\cos\phi\sin\theta}{C_{33}-C_{44}} \right) \hat{k} \\ \hat{u}_{pS} &= \frac{\sin\phi}{n}\hat{\theta} + \frac{\cos\phi\cos\theta}{n}\hat{\phi}\end{aligned}\quad (14)$$

\hat{u}_{pS} is perpendicular to both \hat{k} and the axis of symmetry of the HTI medium (the x -axis).

First-order phase velocities for weak HTI:

$$\begin{aligned}v_p &= v_p^0 [1 + g_{11}(1-n^2)^2 + g_{13}(1-n^2)n^2] \\ v_{qS} &= v_s^0 [1 + g_{66} + \frac{C_{33}}{C_{44}}(g_{11} - g_{13})n^2(1-n^2)] \\ v_{pS} &= v_s^0 [1 + g_{66}(1-n^2)]\end{aligned}\quad (15)$$

The first expression in (15) agrees with the P-wave phase velocity formula derived by Gajewski and Psencik (1996).

First-order group velocities for weak HTI:

$$\begin{aligned}\vec{V}_p &= v_p \hat{k} + 2v_p^0 [(2g_{11}(1-n^2) + g_{13}(2n^2-1)]\cos\phi\sin\theta \\ &\quad (\cos\theta\cos\phi\hat{\theta} - \sin\phi\hat{\phi}) \\ \vec{V}_{qS} &= v_{qS} \hat{k} + 2v_s^0 \left(\frac{C_{33}}{C_{44}} \right) (g_{11} - g_{13}) n (1-2n^2) \cos\phi\sin\theta \\ &\quad \left(-\frac{\cos\theta\cos\phi}{n}\hat{\theta} + \frac{\sin\phi}{n}\hat{\phi} \right) \\ \vec{V}_{pS} &= v_{pS} \hat{k} - 2v_s^0 g_{66} \cos\phi\sin\theta (-\cos\theta\cos\phi\hat{\theta} + \sin\phi\hat{\phi})\end{aligned}\quad (16)$$

Explicit imaging expressions for weak horizontal transverse isotropy

where, v_p , v_{pS} and v_{qS} are the P- and S-wave phase velocities given in (15).

Conclusions

Making use of the fact that the HTI and the VTI systems are representations of the same crystal symmetry class, in two different coordinate systems, we developed a complete set of imaging expressions for weak HTI systems from their well-known VTI counterparts. Our HTI expressions account for propagation of waves in arbitrary directions with respect to the acquisition coordinate system. Therefore, they can be readily incorporated into the multi-component seismic data processing algorithms.

Figures 3 and 4 offer insights into the accuracy of the first-order TI imaging expressions. The figures were generated from the generic data discussed by Schoenberg and Helbig (1997). The exact results were generated from numerical solutions of the Christoffel equation. Since the Schoenberg-Helbig data is not entirely “weak”, the excellent agreement between the approximate and exact results seen in our figures demonstrate the accuracy and robustness of the first order imaging expressions discussed here.

References

Gajewski, D., Psencik, I., 1996, qP wave phase velocities in weakly anisotropic media – perturbation approach: 66th Ann. Internat. Mtg., Soc. Expl. Geophys., Expanded abstracts, 1507-1510.

Lynn, H. B., Bates, C. R., Simon, K., M., and van Dok, R., 1995, The effects of azimuthal anisotropy in P-wave 3-D seismic. 65th Ann. Internat. Mtg. Soc. Expl. Geophysics., Expanded Abstracts, 293-296.

Ohanian V., W.E. Beckham 1992, Depth-variant fracture orientation from multicomponent VSP. 62nd Ann. Internat. Mtg., Soc. Expl. Geophys. Expanded Abstracts 177-180.

Ohanian, V., 1996, Weak transverse isotropy by perturbation theory: 66th Ann. Internat. Mtg., Soc. Expl. Geophys., Expanded Abstracts, 1838-1841.

Ohanian, V., Snyder T. M., and Carcione J., 1997, Mesaverde and Green River shale anisotropies by wavefront folds and interference patterns: 67th Ann. Internat. Mtg., Soc. Expl. Geophys., Expanded Abstracts, 937-940.

Rommel, B. E., 1994, Approximate polarization of plane waves in medium having weak transverse isotropy: Geophysics, 59, 1605-1612.

Schoenberg, M., Helbig, K., 1997, Orthorhombic media: Modeling elastic wave behavior in vertically fractured earth: Geophysics, 62, 1954-1974.

Thomsen, L., 1986, Weak elastic anisotropy: Geophysics, 51, 1954-1966.

Tsvankin, I., 1997, Reflection moveout and parameter estimation for horizontal transverse isotropy: Geophysics, 62, 614-629.

Winterstein, D. F., and Meadows, M. A. 1991a, Changes in shear wave polarization azimuth with depth in Cymric and Railroad Gap oil fields: Geophysics, 56, 1349-136

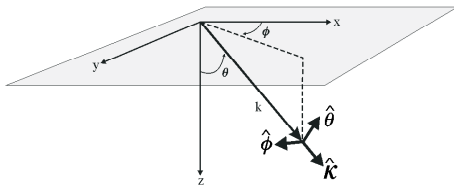


Fig. 1 The acquisition and spherical coordinate systems

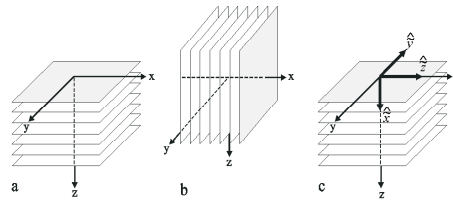


Fig. 2 The configuration of the VTI and HTI systems

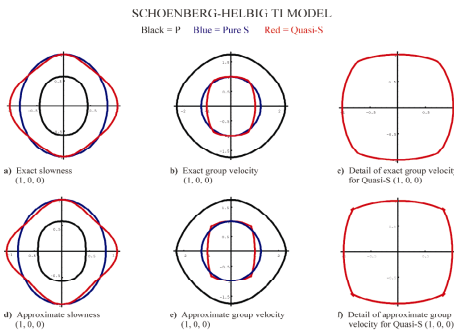


Fig. 3. Exact and approximate slowness and group velocities

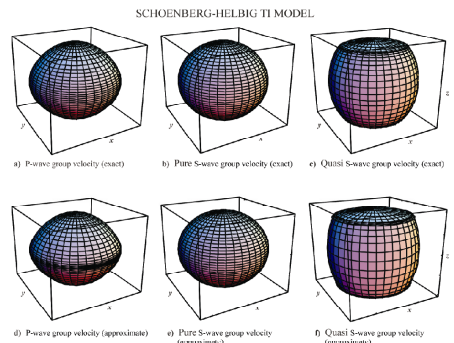


Fig. 4 Exact and approximate group velocity surfaces